Environmental Research 212 (2022) 113182

Contents lists available at ScienceDirect

Environmental Research

journal homepage: www.elsevier.com/locate/envres

Particulate organic nitrates at Mount Tai in winter and spring: Variation characteristics and effects of mountain-valley breezes and elevated emission sources

Jing Chen [a], Xinfeng Wang [a,*], Jun Zhang [a,b], Min Li [a], Hongyong Li [a], Zhiyi Liu [a], Yujian Bi [c], Di Wu [c], Xiangkui Yin [c], Rongrong Gu [a], Ying Jiang [a], Ye Shan [a], Yong Zhao [c], Likun Xue [a], Wenxing Wang [a]

[a] Environment Research Institute, Shandong University, Qingdao, 266237, China
[b] Laboratory of Atmospheric Chemistry, Paul Scherrer Institute (PSI), 5232, Villigen, Switzerland
[c] Taishan National Reference Climatological Station, Tai'an, 271000, China

ARTICLE INFO

Keywords:
Particulate organic nitrates
Variation characteristics
Influencing factors
Mountain-valley breeze
Elevated emission sources

ABSTRACT

Particulate organic nitrates, among the major components of secondary organic aerosols and fine particles, play important roles in regional nitrogen cycle, ozone budget, and cloud condensation nuclei formation. However, the pollution characteristics of particulate organic nitrates at mountain areas and the effects of anthropogenic pollutant transport remain poorly understood. In this study, field sampling and measurements were conducted at a high-elevation mountain site over North China Plain in winter and spring. Total five kinds of particulate organic nitrates in fine particles were determined by ultra-high performance liquid chromatography-electrospray mass spectrometry. The average total concentrations of particulate organic nitrates were 330 ± 121 ng m^{-3} and 247 ± 63 ng m^{-3} in winter and spring. The monoterpene-derived organic nitrates were the dominant components in both seasons with their contribution higher than 70%, accounting for 1.2 ± 0.8% and 2.0 ± 1.0% in organic aerosols in winter and spring, respectively. The significantly higher levels of particulate organic nitrates in winter than spring was ascribed to the strong effects of mountain-valley breezes and coal combustion plumes. The increasing concentrations of NO_x and particulate matters brought by the valley breeze at daytime facilitated the formation of MHN215, OAKN359, and OAHN361, while the rising SO_2 abundance and the sulfate aerosols transported by elevated emission sources affected the formation of MDCN247 at nighttime.

1. Introduction

Organic nitrates, mainly derived from the oxidation of volatile organic compounds (VOCs) in the presence of reactive nitrogen oxides, play a vital part in the tropospheric chemistry, regional nitrogen cycle, and cloud condensation nuclei (CCN) formation. Gaseous organic nitrates are mainly produced from the reactions between VOCs and OH radicals together with NO_x during the daytime and the oxidation of VOCs by NO_3 radicals at nighttime (Perring et al., 2013; Rollins et al., 2012). Following the initial production, gaseous organic nitrates readily turn into the particle phase via gas-particle partitioning or further oxidation during which process the nitrate group is retained. They are eventually removed by dry and wet deposition, or via hydrolysis or photolysis which results in the loss of the nitrate group (Epstein et al., 2014; Takeuchi and Ng, 2019). Therefore, organic nitrates can act as temporary reservoirs of NO_x and influence O_3 budget through the HO_x ($HO_x = OH + HO_2 + RO_2$) cycle and the NO_x cycle (Farmer et al., 2011; Lee et al., 2016; Mao et al., 2013). Organic nitrates are also among the major components of secondary organic aerosols (SOA) and fine particles ($PM_{2.5}$), which aggravate the atmospheric visibility and the air quality (Ayres et al., 2015; Ng et al., 2017). In addition, most of the particulate organic nitrates have strong hygroscopicity because of the containing hydrophilic groups such as nitrate group, hydroxyl group, and carboxyl group, therefore they act as CCN to influence the global radiation balance and regional climate (Tegen and Schepanski, 2018; Twomey et al., 1984; Xu et al., 2015).

Field measurements of particulate organic nitrates were early conducted in North America. Their concentrations were usually in the range

* Corresponding author.
E-mail address: xinfengwang@sdu.edu.cn (X. Wang).

https://doi.org/10.1016/j.envres.2022.113182
Received 9 December 2021; Received in revised form 19 February 2022; Accepted 22 March 2022
Available online 1 April 2022

of 0.01–2.94 μg m^{-3} and varied significantly with locations, time periods, and measurement techniques (Li et al., 2021b). Field observation by Rollins et al. (2013) with thermal dissociation coupled to laser induced fluorescence (TD-LIF) in the San Joaquin Valley in California in summer, 2010 showed average concentrations of 0.20 μg m^{-3} at nighttime and 0.10~0.15 μg m^{-3} during daytime. Moreover, organic nitrates controlled the nocturnal SOA formation with the contribution to organic aerosols up to 27~40%. Fry et al. (2013) observed up to 140 pptv of aerosol-phase organic nitrates using TD-LIF at an urban-affected forest site in Colorado in summer, 2011. In addition, up to 30% of the total organic nitrates existed in the particulate phase at night, while the fraction dropped to less than 10% during daytime. Zare et al. (2018) reported approximately 0.2 ± 0.1 ppbv of organic nitrates in gas and particle phases in Bibb County, Alabama in summer, 2013 and they found that about 52% of the NO_x retained by organic nitrates can be released to the atmosphere again when coupled the observation data with the model simulation results. In recent years, a few studies on particulate organic nitrate were conducted in polluted atmosphere in eastern China. Huang et al. (2021) observed approximately 0.7 μg m^{-3} of particulate organic nitrate in urban Beijing in winter and found that the formation of organic nitrates had a positive relationship with the aerosol liquid water. Zhang et al. (2016) found that organic nitrates could contribute about 21% and 18% of the total particulate nitrate mass in urban Beijing in the biomass burning period and the coal combustion period, respectively by using the AMS-PMF method. In addition, our research group have carried out several observations in different urban and rural sites. Li et al. (2018) reported that the total concentration of five kinds of organic nitrates was 325.4 ± 116.7 ng m^{-3} in urban Jinan in summer, contributing to 1.64 ± 0.34‰ of $PM_{2.5}$, while Zhang et al. (2021) measured maximum of 415 ng m^{-3} in rural Dongying in June 2017. Up to date, most of the field measurements on particulate organic nitrates were carried out in hot seasons in the ground sites. The abundances and variation characteristics at elevated areas in cold seasons remain unclear.

Previous studies have shown that the concentrations of particulate organic nitrates were largely depended on the mixing ratios of precursors and oxidants, aerosol physical and chemical properties, meteorological conditions, and anthropogenic activities. The formation of particulate organic nitrates can be enhanced by increased emissions of VOCs and NO_x (Lee et al., 2019; Li et al., 2021a). In the condition of relatively high humidity, they can form through aqueous reactions and a possible formation pathway was proposed (Xu et al., 2020). Model simulations and laboratory studies also demonstrated the importance of heterogeneous/aqueous reactions for organic nitrates formation (Ng et al., 2017; Northcross and Jang, 2007; Riedel et al., 2015). Besides, several studies have been carried out recently to explore the effects of aerosol acidity on organic nitrates. Rindelaub et al. (2016) proposed an acid-catalyzed hydrolysis mechanism for the α-pinene-derived organic nitrates. Fry et al. (2018) found that coal-burning plumes from thermal power plants which were rich in acidic sulfate aerosols facilitated the formation of organic nitrates at night in their aircraft measurements. Huang et al. (2021) concluded that the increasing aerosol acidity promoted the formation of organic nitrates. In addition, anthropogenic activities also influence the abundances of particulate organic nitrates (Zhang et al., 2021). During biomass burning and coal combustion periods, the average concentration of organic nitrates in submicron particles in Beijing in winter was up to 4.2 μg m^{-3} and 0.8 μg m^{-3}, respectively (Zhang et al., 2016). The above recent findings indicate the strong impacts on particulate nitrate formation from atmospheric conditions and anthropogenic activities. By far, however, more researches are required to understand and confirm the effect degree and the detailed influencing mechanisms.

In this study, $PM_{2.5}$ filter samples were collected at the summit of Mount Tai (Mt. Tai) in winter and spring with simultaneous online measurements of related parameters and subsequent particle chemical analyses. The concentrations and composition of specific organic nitrates were presented. Then, the variation characteristics and influencing factors were analyzed. Finally, the detailed effects and influence mechanisms were explored and discussed. Due to the unique geographical location of Mt. Tai and the complex polluted conditions, the current work can enrich the observation dataset and contribute to a more comprehensive understanding on the sources and formation of particulate organic nitrates.

2. Experiments and methods

2.1. Site description

The sample collection and on-line measurements were conducted in the Taishan National Reference Climatological Station at the summit of Mt. Tai (36.26 N, 117.11 E; 1535 m a.s.l.) in Shandong Province, China. Mt. Tai, the highest peak within the North China plain, is situated in the central part of Shandong Province (Fig. 1). The city of Tai'an, with a population of about 5.5 million, lies 15 km to the south. Although Mt. Tai is a popular tourist spot, the sampling site is located relatively far away from restaurants and temples and is little affected by the nearby anthropogenic activities. Furthermore, the altitude of the measurement site is near the top of the atmospheric boundary layer. As the boundary layer height changes, air pollutants from the ground may be transported to the sampling site with mountain-valley breezes. Due to its unique geographic location, Mt. Tai has been used widely as a sampling site for researches on regional atmospheric pollution and atmospheric chemistry in the past decade (Jiang et al., 2020; Sun et al., 2016; Wang et al., 2017).

2.2. Sample collections and on-line measurements

In total, 118 ambient $PM_{2.5}$ samples were collected from November 26 to December 30, 2017 and from March 9 to April 7, 2018 with a medium-volume sampler (TH-150A, Wuhan Tianhong, China) at a flow rate of 100 L min^{-1}. The samples were collected during daytime and nighttime separately with the daytime samples from 7:00 to 18:30 LT (Local Time, LT = UTC+8) and the nighttime samples from 19:00 to 06:30 LT the next day. In addition, four blank samples were collected before and after each sampling campaign in same conditions except the pump not working. Before sampling, the filters were pre-baked in muff furnace at 600 °C for 4 h to remove organic matters that may be adsorbed on. After the sampling, the filter samples were stored at -20 °C in a freezer for further analysis.

During the sampling periods, related air pollutants and meteorological parameters were also monitored in real time. Trace gases including NO (Model T200U, Advanced Pollution Instrumentation (API), USA), NO_2 (Model T500U, API, USA), SO_2 (Model 43C, Thermo Electron Corporation, USA), O_3 (Model T400, API, USA) and CO (Model 300EU, API, USA) were measured via optical methods at a time resolution of 1 min. Meanwhile, the $PM_{2.5}$ mass concentration was analyzed by the light scattering and beta ray absorption method (SHARP 5030, Thermo Scientific, USA) at a time resolution of 30 min. The meteorological data of relative humidity (RH), temperature (T) as well as wind direction and speed were obtained from the Taishan National Reference Climatological Station.

Inorganic water-soluble ions including Cl^-, NO_2^-, NO_3^-, SO_4^{2-}, Na^+, NH_4^+, K^+, Mg^{2+}, Ca^{2+} were determined by a Monitor for Aerosols and Gases (MARGA, ADI20801, Applikon-ECN, Netherlands) (Wen et al., 2018). The dataset from December 7 to December 23, 2017 were unavailable because of the instrument malfunction.

2.3. Organic nitrate determinations and other chemical analyses

A piece of ~25 cm^2 (one half) was cut from each sample filter and extracted in 15 mL methanol (HPLC grade, Sigma-Aldrich, USA) under sonication for three times. The final extract solution with a volume of

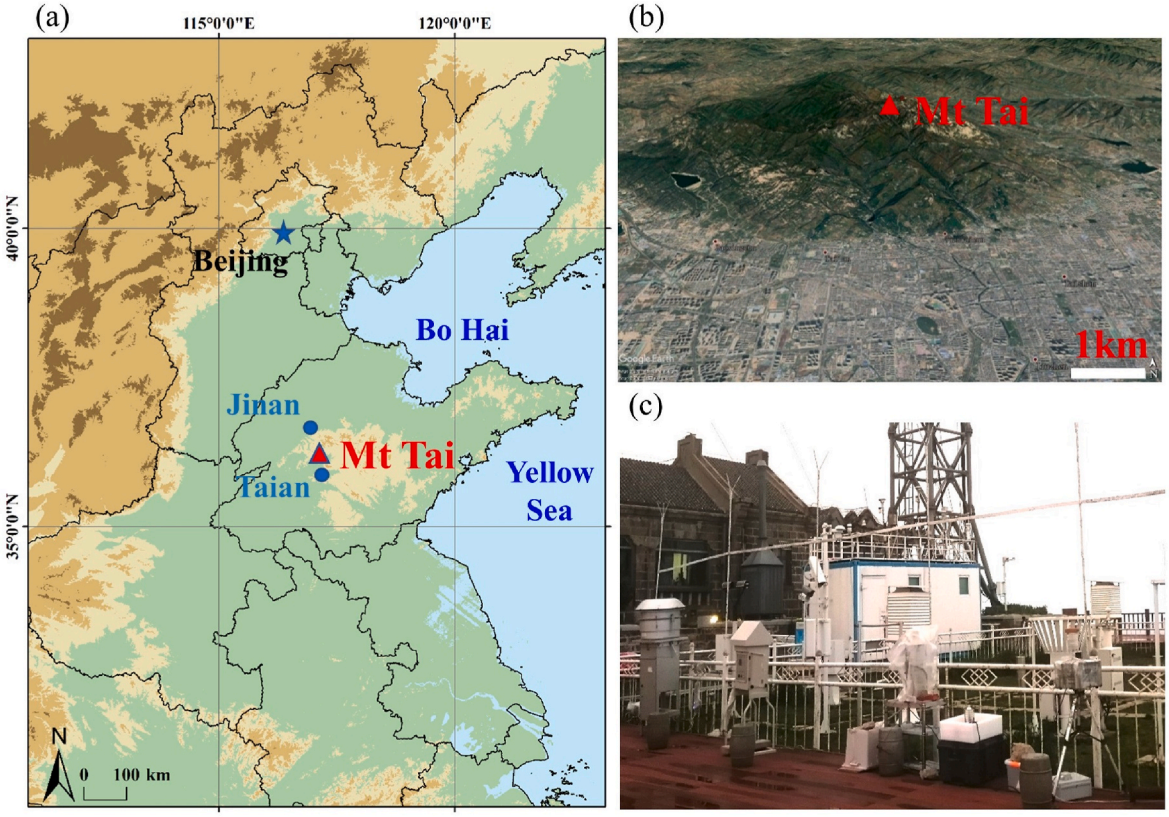

Fig. 1. (a) The location of the observation site (Mt. Tai) deployed in this study, (b) the expanded topographic view of Mt. Tai and the surrounding areas, and (c) a photo of observation site.

approximately 45 mL was kept stationary at 4 °C for 12 h and then concentrated to l mL by rotary evaporation at room temperature. After filtered by the 0.25-μm polytetrafluoroethylene (PTFE) syringe filter, 1.5 mL methanol was added into the concentrated solution and a gentle stream of high purity nitrogen was used to blow it to near-dryness. Finally, 300 μL methanol was added to re-dissolve the residues, and 200 μL was transferred to the brown sample injection bottle for subsequent chemical analysis.

The resulting extracts were analyzed using an ultra-high performance liquid chromatography (UHPLC, Thermo Scientific, USA) coupled to an ion-trap mass spectrometer (MS, ISQEC000LC, Thermo Scientific, USA) equipped with an electrospray ionization (ESI) source operated in positive mode. The analytes were separated by an Atlantis C18 column (2.1 × 15 mm, 2.1 μm, Waters, USA) and the column temperature was set at 24 °C. A gradient elution was performed with methanol (HPLC grade, Sigma-Aldrich, USA; eluent A) and deionized water with 0.1% formic acid (HPLC grade, Sigma-Aldrich, USA; eluent B) at a flow of 0.2 mL min^{-1}. The gradient procedure was set as below: a composition of 30% A and 70% B was maintained for 3 min; it changed to 90% A and 10% B within 10 min and then kept for 3 min; finally it went back to 30% A and 70% B within 0.1 min and hold for 7.9 min. The following five kinds of organic nitrates were identified from $PM_{2.5}$ samples in this study: Monoterpene hydroxyl nitrate (MW = 215, MHN215), Pinene keto nitrate (MW = 229, PKN229), Monoterpene dicarbonyl nitrate (MW = 247, MDCN247), Oleic acid keto nitrate (MW = 359, OAKN359) and Oleic acid hydroxyl nitrate (MW = 361, OAHN361). Two surrogate standards, 2-Hydroxy-3-pinanone (GC-grade, TCI, Japan) for MHN215, PKN229 and MDCN247 and Ricinoleic (Analytical Reagent, Sigma-Aldrich, USA) for OAKN359 and OAHN361, were selected to approximately quantify the contents of the five kinds of organic nitrates based upon similar molecular structures and close retention time (Li et al., 2018). The recoveries of the two surrogate standards were 74.4% and 77.8%, respectively. The structures and retention time of the five kinds of quantified organic nitrates as well as the two surrogate standards used for the quantification are listed in Table A1. The standard curves of the two surrogate standards ($r^2 > 0.99$) are depicted in Fig. A1. The signals of the blank samples were under or near the detection limits and thus were not subtracted from the sample signals when performing the quantification. More details about the identification of organic nitrates can be found in (Li et al., 2018).

In addition, a ~2 cm^2 circular piece was poked from each sample filter to analyze the contents of organic carbon (OC) and elemental carbon (EC) using a semi-continuous OCEC carbon aerosol analyzer (Sunset Laboratory, USA). Methane in helium was used as internal standard and calibrations were performed with different concentrations of sucrose solutions to ensure accurate and reliable analyzing results. The concentrations of primary organic carbon (POC) and secondary organic carbon (SOC) were calculated via the EC tracer method (Dong et al., 2020; Turpin and Huntzicker, 1995). The content of OM is approximately estimated from the OC content:

$$OM = f_{OM/OC} \times OC \quad (1)$$

where $f_{OM/OC}$ is the proportional coefficient between OM and OC and 2.07 was selected for this study according to the previous field study (Yao et al., 2016).

The ISORROPIA-II thermodynamic model was applied to estimate liquid water content (LWC) and the pH value of the fine particles based on the equation below (Fountoukis and Nenes, 2007):

$$pH = -lg\left(\frac{1000[H^+_{air}]}{LWC}\right) \quad (2)$$

where $[H^+_{air}]$ is the concentration of H^+ ion in liquid phase and LWC is the value of liquid water content which are derived from the model with units of μg m^{-3}.

3. Results and discussion

3.1. Concentrations and composition

To understand the abundances and seasonal differences of particulate organic nitrates, the concentrations of the five specific organic nitrates as well as related trace gases and meteorological parameters observed at Mt. Tai in winter and spring were compared (as shown in Table 1). The average concentrations of MHN215, PKN229, MDCN247, OAKN359 and OAHN361 in winter were 107.8 ± 60.1, 90.5 ± 56.2, 32.7 ± 22.6, 25.4 ± 19.1 and 62.7 ± 36.0 ng m^{-3} (mean ± standard deviations), respectively, while were a little lower in spring with values of 104.8 ± 26.8, 64.6 ± 17.3, 15.2 ± 11.8, 21.2 ± 12.1, and 41.5 ± 30.7 ng m^{-3}, respectively. The average total concentration of the five organic nitrates (ΣONs) was 330 ± 121 ng m^{-3} in winter, accounting for 1.0 ± 0.6% of the $PM_{2.5}$ mass concentration, with a maximum contribution of 3.8% at the nighttime of December 8, 2017. The average concentration of ΣONs was 247 ± 63 ng m^{-3} in spring, corresponding to 1.0 ± 0.9% of the $PM_{2.5}$ mass concentration, with a maximum contribution of 4.2% at the daytime of March 12, 2018. The relatively high concentrations of particulate organic nitrates and the notable fractions in $PM_{2.5}$ at the Mt. Tai confirm that organic nitrates are important component of fine particulate matters.

Compared with the particulate organic nitrate concentrations in other locations around the world (Table 2), the concentrations of ΣONs observed at Mt. Tai are comparable with those at the mountain site in Colorado, United States where is characterized by large biogenic emissions and limited anthropogenic influence (Fry et al., 2013). They are higher than those found at the forest sites in Finland and in California, United States (Kortelainen et al., 2017; Rollins et al., 2013), but lower than those at a suburban site in Netherlands (Kiendler-Scharr et al., 2016). The differences in the abundances of particulate organic nitrates among different locations are mainly caused by the different location characteristics and atmospheric environments and are also related to the different detection techniques. When compared with our previous measurements via the same method of UHPLC-MS, the abundances of particulate organic nitrates at Mt. Tai are found similar to the concentrations in urban and rural sites in Shandong and Beijing, suggesting generally high levels of particulate organic nitrates over the North China Plain (Li et al., 2018; Zhang et al., 2020, 2021).

As demonstrated in Table 1, the concentration of ΣONs had obvious seasonal difference, with the average value in winter was 1.3 times as high as that in spring ($p < 0.01$). With examination of the concentrations of related pollutants and meteorological parameters, it is noticed that the average concentrations of NO_x (4.0 ± 3.3 ppbv) and SO_2 (3.7 ± 2.8 ppbv) in winter were significantly higher than those in spring (2.2 ± 1.3 ppbv for NO_x and 1.7 ± 1.2 ppbv for SO_2) ($p < 0.01$). An opposite seasonal pattern was found for the oxidant ozone (49.2 ± 11.1 ppbv in winter vs. 65.4 ± 12.2 ppbv in spring) ($p < 0.01$), while the concentrations of $PM_{2.5}$ were similar during the two seasons (41.3 ± 22.5 μg m^{-3} for winter and 37.3 ± 20.4 μg m^{-3} for spring). The concentrations of OC and EC in winter were almost as twice as those in spring (10.6 ± 4.5 μg m^{-3} and 2.4 ± 1.2 in winter vs. 5.2 ± 2.1 and 1.5 ± 0.8 μg m^{-3} in spring for OC and EC, respectively). Considering that there were rare local anthropogenic emissions near the sampling site at Mt. Tai, the relatively higher concentrations of organic nitrates in winter are probably associated with the transport and aging processes of air pollutants emitted from anthropogenic activities in urban areas.

The proportions of each species to the ΣONs in $PM_{2.5}$ samples are illustrated in Fig. 2. Among the five organic nitrates, no matter in winter or spring, MHN215 was the most abundant component, followed by PKN229 and OAHN361. The proportions of MDCN247 and OAKN359 were relatively small, with the contributions averagely no more than 10%. The MDCN247 concentration was a little higher than OAKN359 in winter, while lower than OAKN359 in spring. The highest proportion of MHN215, with an average of 34% in winter and 42% in spring at Mt. Tai, is consistent with previous filed measurements (Dinkelacker and Pandis, 2021; Zhang et al., 2021), mainly due to the larger emissions of monoterpenes. The total proportion of organic nitrates derived from monoterpenes including MHN215, PKN229, and MDCN247 was approximately 75% in both winter and spring, contributing 1.2 ± 0.8% and 2.0 ± 1.0% to organic aerosols in winter and spring, respectively. It is much higher than that from the oleic acid (OAKN359+OAHN361). It indicates that biogenic volatile organic compounds were the most important precursors of particulate organic nitrates at Mt. Tai. Previous researches have shown that the abundances of monoterpenes in winter are not very low (Cheng et al., 2018; Ding et al., 2016). In addition to the biogenic emissions, they can also be emitted from anthropogenic sources such as industrial production (Cheng et al., 2018), vehicle exhausts (Dai et al., 2010), and biomass burning (Andreae et al., 2019). In addition, the relative abundance of MDCN247 exhibited visible difference between the two seasons, with the proportion in winter almost twice as high as that in spring. The details reason for the seasonal difference in the MDCN247 proportion will be discussed later in Section 3.4.

Table 1
The concentrations of five kinds of organic nitrates and $PM_{2.5}$, related trace gases, and meteorological parameters at Mt. Tai (average ± standard deviation).

Species/parameter	Winter	Spring
MHN215 (ng m^{-3})	107.8 ± 60.1	104.8 ± 26.8
PKN229 (ng m^{-3})	90.5 ± 56.2	64.6 ± 17.3
MDCN247(ng m^{-3})	32.7 ± 22.6	15.2 ± 11.8
OAKN359 (ng m^{-3})	25.4 ± 19.1	21.2 ± 12.1
OAHN361 (ng m^{-3})	62.7 ± 36.0	41.5 ± 30.7
ΣONs (ng m^{-3})	330.5 ± 120.8	247.4 ± 63.5
$PM_{2.5}$ (μg m^{-3})	41.3 ± 22.5	37.3 ± 20.4
ΣONs/$PM_{2.5}$ (%)	1.0 ± 0.6	1.0 ± 0.9
OC (μg m^{-3})	10.6 ± 4.5	5.2 ± 2.1
EC (μg m^{-3})	2.4 ± 1.2	1.5 ± 0.8
POC (μg m^{-3})	4.9 ± 2.4	2.8 ± 1.6
SOC (μg m^{-3})	5.8 ± 2.5	2.4 ± 1.4
CO (ppmv)	0.38 ± 0.16	0.40 ± 0.12
SO_2 (ppbv)	3.7 ± 2.8	1.7 ± 1.2
NO (ppbv)	0.6 ± 1.0	0.2 ± 0.2
NO_2 (ppbv)	3.4 ± 2.4	2.0 ± 1.1
NO_x (ppbv)	4.0 ± 3.3	2.2 ± 1.3
O_3 (ppbv)	49.2 ± 11.1	65.4 ± 12.2
T (°C)	-8.1 ± 4.1	8.4 ± 6.0
RH (%)	46.5 ± 17.4	65.3 ± 22.9

3.2. Variation characteristics and influencing factors

Fig. 3 depicts the time series of the concentrations of organic nitrates, mixing ratios of gaseous pollutants, and meteorological conditions during the two sampling periods. As shown, the maximum concentration of ΣONs was observed at the nighttime of December 13 in winter and March 18 in spring, up to 774 ng m^{-3} and 428 ng m^{-3}, respectively. The PKN229 concentration also reached its maximum value of 353 ng m^{-3} at the nighttime of December 13 and the concentrations of both MHN215 and PKN229 at the nighttime of March 18 reached their maximum values of 217 ng m^{-3} and 107 ng m^{-3}, respectively. With examination of meteorological parameters, the humidity in these two pollution cases were relatively high, with the RH up to 88% and 97%, respectively, implying a potential heterogeneous or aqueous formation pathway for organic nitrates. Previous researches have confirmed that aqueous chemistry of semi-volatile organic compounds resulted in efficient formation of secondary organic aerosols in the condition of high humidity (Hu et al., 2016). High relative humidity could enhance the aqueous phase reactions and the monoterpene derived SOA formation in the atmospheric particle (Mahilang et al., 2021). Field study at a forest site has shown that aerosol liquid water could promote the formation of water-soluble organic nitrogen in aerosols (Xu et al., 2020). As shown by the predictions from ISORROPIA-II thermodynamic model, liquid water could appear when the RH exceeded 20%. With the increasing of the RH

Table 2
Concentrations of particulate organic nitrates (ONs) from field observations in previous studies and this study (units: ng m^{-3}).

Location	Site type	Sampling period	Species	Measurements	Concentration	Reference
Colorado, USA	montane site	July–Aug. 2011	particulate ONs	TD-LIF	10~80 pptv	Fry et al., (2013)
California, USA	suburban site	May–June 2010	particulate ONs	TD-LIF	25~250	Rollins et al., (2013)
Finland	forest site	Mar.–Apr. 2011	particulate ONs	HR-TOF-AMS	33 ± 57	Kortelainen et al., (2017)
Netherlands	suburban site	May 2008 Oct. 2008	particulate ONs	HR-TOF-AMS	average 520 (200~1800)	Kiendler-Scharr et al., (2016)
Hebei, China	rural site	Dec. 2018	particulate ONs	HR-TOF-AMS	500~900	Huang et al., (2021)
Dongying, China	rural site	Jan. 2018	5 ONs, $C_{10}H_{17}NO_7S$	HPLC-MS	113~415	Zhang et al., (2021)
Shenzhen, China	urban site	2015–2016	particulate ONs	HR-TOF-AMS	120~530	Yu et al., (2019)
Jinan, China	urban site	June 2016	[a]5 ONs, $C_{10}H_{17}NO_7S$	HPLC-MS	71~1338	Li et al., (2018)
Beijing, China	urban site	Jan. 2018	[a]5 ONs, $C_{10}H_{17}NO_7S$	HPLC-MS	126~528	Zhang et al., (2020)
Mt Tai	montane site	Nov.–Dec. 2017	[a]5 ONs	HPLC-MS	122~774	(This study)
Mt Tai	montane site	Mar.–Apr. 2018	[a]5 ONs	HPLC-MS	153~428	(This study)

[a] 5 ONs refer to $C_{10}H_{17}NO_4$, $C_{10}H_{15}NO_5$, $C_{10}H_{17}NO_6$, $C_{18}H_{33}NO_6$, and $C_{18}H_{35}NO_6$ in this study.

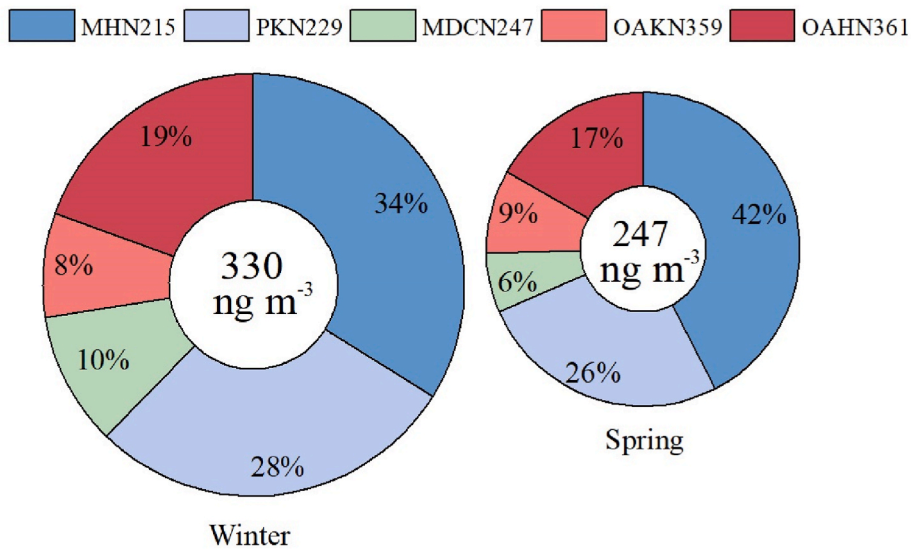

Fig. 2. The proportions of the five kinds of organic nitrates at Mt Tai. The values in the center of the rings represent the average concentration of ΣONs in winter and spring, respectively.

from 20% to 70%, the LWC increased slowly. Nevertheless, when the RH was greater than 70%, the LWC increased rapidly with the maximum up to 755 μg m^{-3}. In these two cases, in the condition of high humidity, it is possible that liquid water appeared on the surface of fine particles and promoted the uptake of gas-phase water-soluble pollutants and the subsequent aqueous reactions, and therefore probably enhanced the formation of particulate organic nitrates. In addition, the abundant liquid water also facilitated the gas-particle partitioning of organic nitrates in these two pollution cases.

The second highest concentration of ΣONs during the winter sampling period, 646 ng/m^3, was observed at the daytime of December 1, accompanied with the appearance of the maximum MHN215 concentration of 359 ng/m^3. In this winter pollution case, high concentrations of NO_x and CO were noticed in the levels of 12.4 ppbv and 0.90 ppmv, respectively, demonstrating the potential transport of polluted air masses from urban emission sources. Besides, the maximum SO_2 concentration was up to 10.2 ppbv and the equivalent molar ratio of sulfate in anions increased from 19% to 46%. The relative humidity was in the range from 29% to 57%. In addition, based on the predictions by ISORROPIA-II thermodynamic model, the average LWC reached 8.1 ± 6.7 μg m^{-3} and the average pH value was as low as 2.2 ± 1.1, which meet the conditions in which acid-catalyzed aqueous reactions can take place. Therefore, it is likely that the coal combustion plume created required conditions for the occurrence of acid-catalyzed aqueous reactions and affected the formation of particulate organic nitrates in this pollution case. During the spring sampling period, the second highest concentration of ΣONs appeared at the daytime of March 13, in the level of 400 ng/m^3. In the spring, the OAHN361 concentration reached its maximum of 134 ng/m^3 and the ozone concentration was also relatively high – up to 74.6 ppbv. Furthermore, compared with other pollution cases in spring, the ambient temperature at the daytime of March 13 (10 °C) was comparatively high. The intense photochemical oxidation activity in spring possibly enhanced formation of organic nitrates.

Further analysis was performed by grouping the sample cases according to the concentration of ΣONs. During the winter sampling period, there were 20 high-ΣONs cases with the concentration higher than 350 ng/m^3, in which MHN215, PKN229, and OAKN359 accounted for very high proportions. It is found that the concentrations of NO_x and CO for high-ΣONs group were significantly higher than those for low-ΣONs group (with ratios of 1.5 and 1.4, respectively; $p < 0.01$). In addition, most of these high-ΣONs cases occurred at daytime with the wind from the south where the urban Tai'an is located. The elevated particulate organic nitrates and trace gases at the daytime under southern wind conditions are ascribed to the pollutant transport and the subsequent aging processes caused by valley breezes. Detailed analyses and discussion on the impacts of mountain-valley breeze will be seen in Section 3.3. During the spring sampling period, there were only 3 high-ΣONs cases with the concentration above 350 ng/m^3 and 24 moderately high-ΣONs cases with the concentration larger than 250 ng/m^3. Interestingly, high and moderately high-ΣONs cases presented significantly

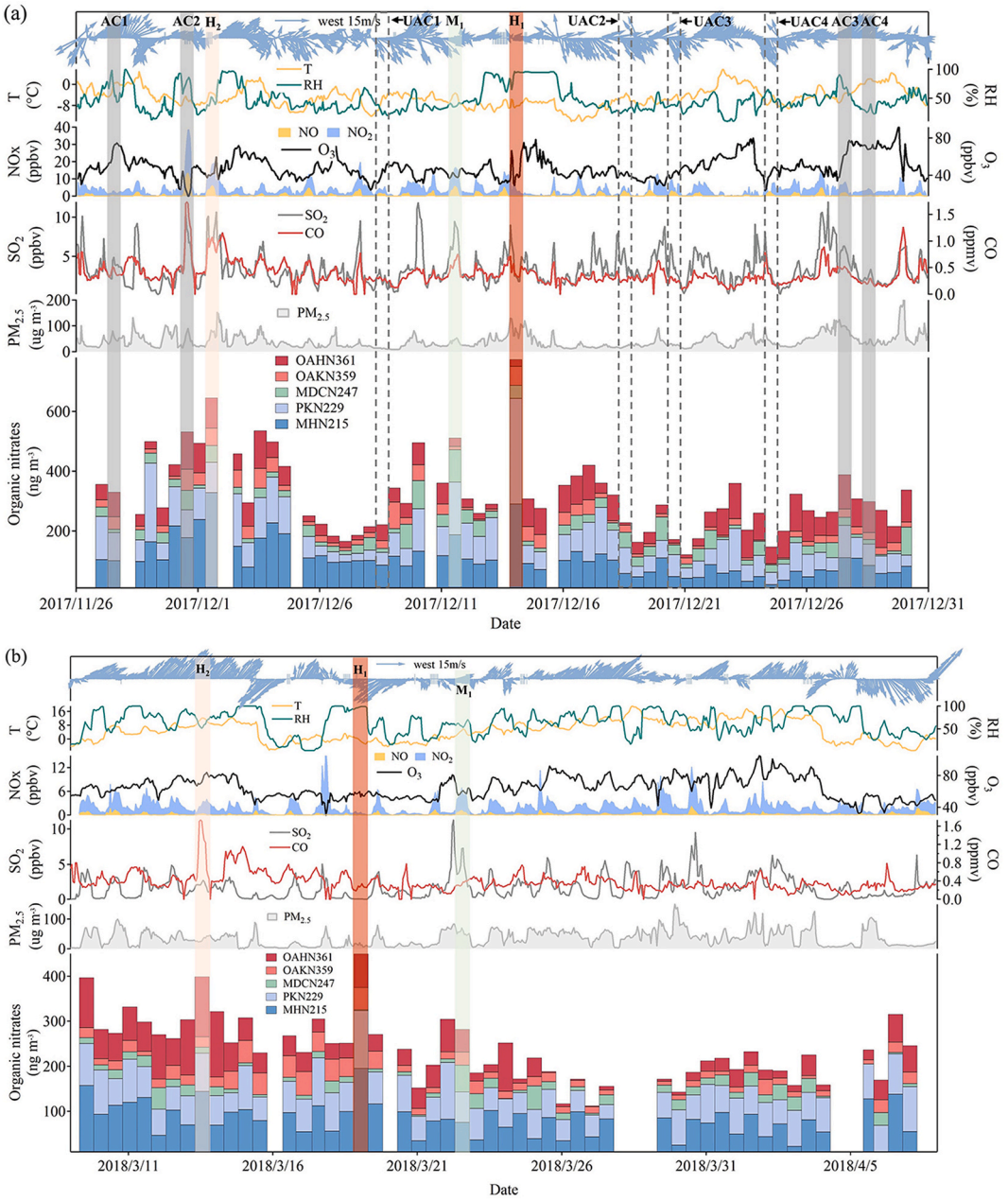

Fig. 3. Time series for the concentrations of five organic nitrates and $PM_{2.5}$, related trace gases, and meteorological data measured at Mt. Tai in winter (a) and spring (b) campaigns. AC and UAC stand for the affected cases and unaffected cases by mountain-valley breezes. H_1 and H_2 refer to the maximum and sub-high concentration of ΣONs. M_1 refers to the maximum concentration of MDCN247.

higher proportions of organic nitrates in secondary organic aerosols than low-ΣONs cases (with the average carbon ratio of 9.2% v.s. 5.4%; $p < 0.01$), indicating enhanced secondary formation of particulate organic nitrates in pollution cases in spring.

As for the organic nitrate MDCN247, it reached its maximum concentration of 108 ng/m^3 and 60 ng/m^3 on the daytime of December 11, 2017 and March 22, 2018. With examination of atmospheric conditions in these two pollution cases, it was found that the corresponding SO_2 concentrations are rather high, up to 6.6 ppbv and 4.7 ppbv respectively, far higher than the average levels of 3.7 ppbv in winter and 1.7 ppbv in spring. Therefore, it is speculated that the rich SO_2 or the coal combustion plumes affected the formation of MDCN247. Detailed analyses on the affected formation of MDCN247 will be shown in Section 3.4.

3.3. Transport via mountain-valley breeze at daytime

As a typical mountain site, Mt. Tai is apparently affected by mountain-valley breezes (Jiang et al., 2020; Sun et al., 2016). As shown in Fig. 3, the spikes in the concentrations of CO, NO_x, SO_2 and $PM_{2.5}$ were frequently encountered during the sampling period in winter, indicating the transport of polluted plumes to the mountain top. These pollutants often presented well-defined diurnal patterns with a daytime concentration peak, which is consistent with the characteristic of the mountain-valley breeze. To understand the influence of mountain-valley breezes on the concentrations of particulate organic nitrates at Mt. Tai at daytime in winter, the daytime samples with and without apparent influences of mountain-valley breezes were selected based on the following three criteria. The first criterion is that the CO concentration increased obviously at the daytime (usually with a peak in the

afternoon). Since CO has a long atmospheric lifetime and is relatively stable in the atmosphere, the notable increase in CO concentration usually means the transport of polluted air masses. The second criterion is that the RH increased at noon or afternoon. Along with the transport of warm air from the ground surface to the summit of the mountain, the RH will increase due to the decrease in the temperature of the air mass. The third criterion is that the wind came from the southern part. As shown in the topographic map of Mt. Tai in Fig. 1, Tai'an city is located in the south and at the foot of the mountain. Therefore, air pollutants in urban Tai'an are readily transported to the sampling site at the summit of Mt. Tai under the condition of south winds. When the southern wind prevails, the concentrations of CO and other pollutants usually presented an obvious increase during the daytime, and the RH also showed an increase. In contrast, the diurnal profile of CO and RH mostly changed gently during the daytime when the winds from other directions dominated, due to the suppression of mountain-valley breezes.

According to the above three criteria, four "affected cases" (ACs; the daytime of November 27 and 30, and December 27 and 28) and four "unaffected cases" (UACs; the daytime of December 8, 18, 20, and 24) were selected (marked in Fig. 3; solid rectangles represent ACs and dotted rectangles represent UACs). As shown in Fig. 3, in the affected cases, the wind mostly came from the south or southwest and the CO concentration exhibited apparent daytime increases, indicating obvious influence from the mountain-valley breezes at the daytime. Nevertheless, in the unaffected cases, the wind mainly came from the north or northwest, the CO concentration and the RH almost kept stable. Fig. 4 compares the concentrations and compositions of particulate organic nitrates in affected and unaffected cases. Overall, the concentrations of total organic nitrates and most individual organic nitrates (except MDCN247) in affected cases were significantly higher than those in unaffected cases. Particularly, the average concentration of total organic nitrates, MHN215, OAKN359, and OAHN361 in affected cases were 2.0, 2.2, 2.7, and 3.2 times as high as those in unaffected cases. In addition, compared with unaffected cases, the proportions of MHN215, OAKN359 and OAHN361 in affected cases increased, while the fractions of PKN229 and MDCN247 decreased. In particular, the proportions of oleic acid-derived organic nitrates (OAKN359 and OAHN361), the precursor of which is a major component of cooking oil, increased from 25% to 38%. The above results demonstrate the large impact of mountain-valley breezes on the abundances and composition of particulate organic nitrates in winter. During the daytime, the valley breeze from the southern directions brought a large quantity of air pollutants to the mountain summit, not only increasing the concentrations of organic nitrates, but also changing their chemical composition.

Under the influence of mountain-valley breezes, the increases in the proportions of MHN215, OAKN359 and OAHN361 are mainly attributed to the enhanced formation of them in the polluted urban plumes. Compared with PKN229 and MDCN247, the precursors of MHN215 are more widely available, including α-pinene, β-pinene and limonene, etc., and thus form via more formation pathways (Fry et al., 2009; Perraud et al., 2010). Furthermore, the oxidation degree of PKN229 (containing carbonyl functional group) and MDCN247 (containing dicarbonyl functional group) are higher than MHN215 (containing hydroxyl functional group). Therefore, in the polluted urban plumes, along with the increasing concentrations of precursors during the short-distance transport, MHN215 is more inclined to form (Zhang et al., 2021). As for OAKN359 and OAHN361, since their precursor oleic acid is produced primarily from human cooking activities, mountain-valley breezes transported a large amount of urban pollutants including rich oleic acids, finally resulting in increased generation of oleic acid derived organic nitrates.

3.4. Impacts from elevated source at nighttime

Surrounding the Mt. Tai, a number of coal-fired industries, such as thermal power plants, cement plants, and steel plants, are distributed in the urban and suburban areas of several cities including Tai'an in the south, Jinan in the North, Liaocheng in the west, and Zibo in the east. During the nighttime of the sampling period in winter, as shown in Fig. 5, the MDCN247 exhibited good correlations with POC ($r = 0.83$, $p < 0.01$), SO_2 ($r = 0.72$, $p < 0.01$), NO_2 ($r = 0.78$, $p < 0.01$) and moderate correlations with SOC ($r = 0.63$, $p < 0.01$), CO ($r = 0.67$, $p < 0.01$), and the product of NO_2 and ozone (NO_2*O_3) ($r = 0.69$, $p < 0.01$). In addition, the MDCN247 concentration at nighttime presented a consistent trend with SO_2, NO_2, and NO_2*O_3 (shown in Fig. 6). Moreover, backward trajectory analysis shows that when elevated concentrations of MDCN247 and SO_2 concurrently appeared (*e.g.*, at the nighttime of December 9, 19, 21, 23, and 26), the air masses passed over the regions with intensive industries and climbed to arrive to the sampling site at the summit of Mt. Tai (shown in Fig. A2), as reported in the previous study by (Wang et al., 2017). As well known, SO_2 is a good indicator for coal combustion plumes and coal combustion also emits a large quantity of NO_x and organic matters. Additionally, the product of NO_2 and ozone, representing the source strength of NO_3 radical and N_2O_5, stands for the nocturnal oxidation capacity. It together with the SOC relate to the secondary formation of organic aerosols. The above results suggest that

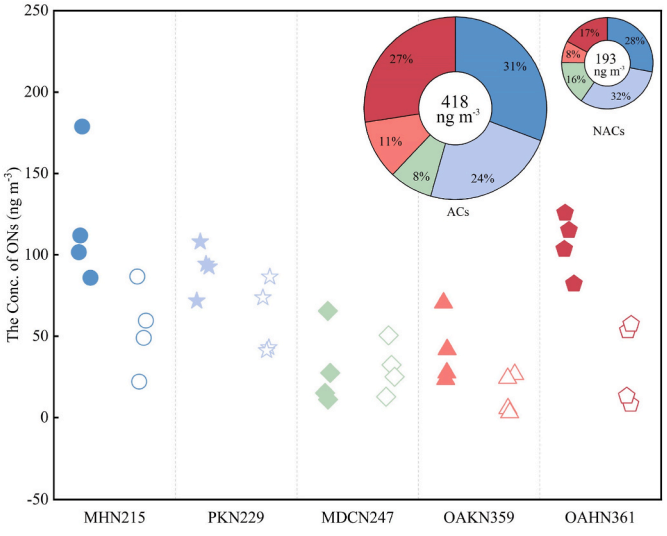

Fig. 4. Comparisons between ACs and UACs in the concentrations and compositions of organic nitrates. Hollow markers denote UACs, while the solid markers denote ACs. The values in the center of the rings represent the average concentrations of ΣONs for ACs and UACs, respectively.

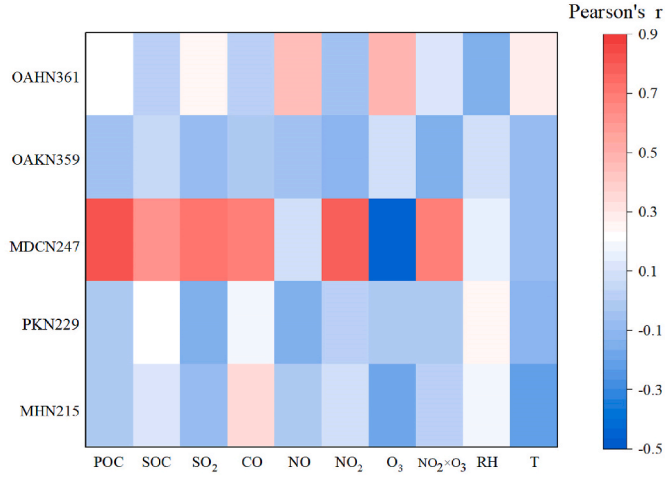

Fig. 5. Correlations of five kinds of organic nitrates with different parameters including POC, SOC, SO_2, CO, NO, NO_2, O_3, $NO_2 \times O_3$, RH, and T by heat map.

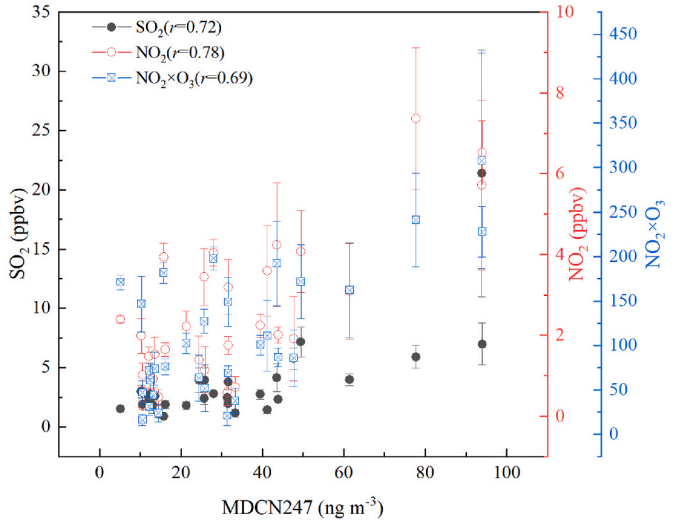

Fig. 6. Scatter plots between the concentrations of MDCN247 and SO_2, NO_2, and the product of NO_2 and O_3 (error bar represents 1/2 standard deviation).

the elevated MDCN247 concentrations at nighttime in winter was strongly associated with the coal-combustion emission sources and was linked to secondary formation processes. In winter, due to the very large consumption of coal for heating purpose and power generation, the concentration and proportion of MDCN247 in winter were much higher than those in spring. The enhanced formation of isoprene-derived nitrates has also been reported in power plant plumes based on aircraft observations in the southeast of the United States by (Fry et al., 2018). Note that no significant correlation was found between the MDCN247 concentration and the ambient RH, indicating that other factors such as concentrations of precursors and oxidants and aerosols properties instead of the humidity (or the aerosol water content) dominated the formation of MDCN247.

Previous studies have shown that the plumes emitted from coal-fired power plants is highly acidic and is favourable for secondary organic aerosol formation. The coal combustion plume contains sulfuric acid aerosols and the high concentration of SO_2 is readily oxidized to produce sulfuric acid. Sulfuric acid aerosols provide seed aerosols and acid-catalyzed reactions to promote the generation of secondary organic aerosols including organic nitrates (Hewitt, 2001; Hlawiczka et al., 2016). Han et al. (2016) find that organic nitrates can be generated through acid-catalyzed reactions, or the acidic condition contributes to the partitioning of gaseous organic nitrates into particle phase. Therefore, it is possible that the high concentrations of acidic aerosols in the coal-combustion plumes affected the formation of MDCN247 when the plumes transported to the sampling site at Mt. Tai.

Furthermore, the latest Master Chemical Mechanism (MCM, http://mcm.leeds.ac.uk/MCM/, version3.3.1) shows that SO_2 can directly react with Criegee intermediates (CIs) which derived from limonene and ozone, and then react with NO_3 to form MDCN247. CIs are important oxidants in troposphere and have significant contribution to global SO_2 oxidation and atmospheric oxidation capacity (Huang et al., 2015; Khan et al., 2018; Novelli et al., 2017). Theoretical studies, field observations, and laboratory simulations also confirm the quite rapid reactions between SO_2 and CIs and the rate coefficients are up to 10^{-11} – 10^{-13} cm^3 $molecules^{-1}$ s^{-1} (Berndt et al., 2012; Jiang et al., 2010; Welz et al., 2012). Therefore, the reactions between SO_2 and CIs in the coal-combustion plumes can affect the formation of MDCN247 during the transport to a certain extent. When compared with the major precursors of α-pinene and β-pinene for MHN215 and PKN229, the reaction rates between MDCN247's main precursor limonene and ozone and the subsequent reaction rate of the produced CIs with SO_2 are much faster than pinenes (McGlynn et al., 2021; Ye et al., 2018). Therefore, only MDCN247 experienced remarkable formation in coal combustion plumes and exhibited strong correlations with SO_2. Further investigations are required to obtain comprehensive understanding on the roles of SO_2 in the formation of different organic nitrates in the future.

4. Conclusions

To understand the pollution characteristics of particulate organic nitrates and the major sources and influencing factors at high altitude in North China Plain, fine particle samples were collected at the summit of Mt. Tai (1534 m a.s.l.) in the winter of 2017 and the spring of 2018 and five kinds of particulate organic nitrates were determined by UHPLC/MS. The average total concentrations of particulate organic nitrates in winter and spring were 330 ± 121 and 247 ± 63 ng m^{-3}, respectively and were significantly higher in winter than in spring. MHN215, PKN229, and OAKN361 were the dominant species in the measured particulate organic nitrates, with the total contribution above 80%. The high levels of particulate organic nitrates are mainly attributed to the heterogeneous or aqueous reactions under high humidity, the transport and aging processes of urban or industrial plumes, and the oxidation processes in the presences of photochemical oxidants. Comparative analysis and case analyses show that mountain-valley breezes had a substantial impact on the abundance and composition of particulate organic nitrates at daytime, leading to increases in both concentrations and fractions of MHN215, OAKN359 and OAHN361. In addition, the good correlation and consistent trends between MDCN247 and SO_2 suggest that the transport of coal-combustion plumes affected the formation of MDCN247 through the acid-catalyzed reactions by acidic sulfate aerosols and the fast reactions between SO_2 with Criegee intermediates. This study highlights the large impacts of transport of anthropogenic pollutant on the formation of particulate organic nitrates at mountain site. More in-depth field and laboratory studies are needed to better understand the detailed formation pathways.

Declaration of competing interest

The authors declare that they have no known competing financial interests or personal relationships that could have appeared to influence the work reported in this paper.

Acknowledgements

This work was supported by the National Key Research and Development Program of China (no. 2020YFF01014503), the National Natural Science Foundation of China (no. 41775118), the Natural Science Foundation of Shandong Province (no. ZR2020YQ30), and the Youth Innovation Program of Universities in Shandong Province (2019KJD007) and received financial support from Shandong University (grant no. 2020QNQT012). The authors would like to thank the Mount Tai Meteorological station for providing meteorological data and the NOAA Air Resource Laboratory for providing the HYSPLIT model.

Appendix A. Supplementary data

Supplementary data to this article can be found online at https://doi.org/10.1016/j.envres.2022.113182.

References

Andreae, M.O., 2019. Emission of trace gases and aerosols from biomass burning - an updated assessment. Atmos. Chem. Phys. 19, 8523–8546. https://doi.org/10.5194/acp-19-8523-2019.

Ayres, B.R., Allen, H.M., Draper, D.C., Brown, S.S., Wild, R.J., Jimenez, J.L., Day, D.A., Campuzano-Jost, P., Hu, W., de Gouw, J., Koss, A., Cohen, R.C., Duffey, K.C., Romer, P., Baumann, K., Edgerton, E., Takahama, S., Thornton, J.A., Lee, B.H., Lopez-Hilfiker, F.D., Mohr, C., Wennberg, P.O., Nguyen, T.B., Teng, A., Goldstein, A. H., Olson, K., Fry, J.L., 2015. Organic nitrate aerosol formation via NO_3 + biogenic

volatile organic compounds in the southeastern United States. Atmos. Chem. Phys. 15, 13377–13392. https://doi.org/10.5194/acp-15-13377-2015.
Berndt, T., Jokinen, T., Mauldin, R.L., Petaja, T., Herrmann, H., Junninen, H., Paasonen, P., Worsnop, D.R., Sipila, M., 2012. Gas-phase ozonolysis of selected olefins: the yield of stabilized Criegee intermediate and the reactivity toward SO_2. J. Phys. Chem. Lett. 3, 2892–2896. https://doi.org/10.1021/jz301158u.
Cheng, X., Li, H., Zhang, Y.J., Li, Y.P., Zhang, W.Q., Wang, X.Z., Bi, F., Zhang, H., Gao, J., Chai, F.H., Lun, X.X., Chen, Y.Z., Gao, J., Lv, J.Y., 2018. Atmospheric isoprene and monoterpenes in a typical urban area of Beijing: pollution characterization, chemical reactivity and source identification. J. Environ. Sci. 71, 150–167. https://doi.org/10.1016/j.jes.2017.12.017.
Dai, T.Y., Wang, W., Ren, L.H., Chen, J.H., Liu, H.J., 2010. Emissions of non-methane hydrocarbons from cars in China. Sci. China Chem. 53, 263–272. https://doi.org/10.1007/s11426-010-0002-6.
Ding, X., Zhang, Y.Q., He, Q.F., Yu, Q.Q., Shen, R.Q., Zhang, Y.L., Zhang, Z., Lyu, S.J., Hu, Q.H., Wang, Y.S., Li, L.F., Song, W., Wang, X.M., 2016. Spatial and seasonal variations of secondary organic aerosol from terpenoids over China. J. Geophys. Res. Atmos. 121, 14661–14678. https://doi.org/10.1002/2016jd025467.
Dinkelacker, B.T., Pandis, S.N., 2021. Effect of chemical aging of monoterpene products on biogenic secondary organic aerosol concentrations. Atmos. Environ. 254 https://doi.org/10.1016/j.atmosenv.2021.118381.
Dong, S.W., Wang, X.F., Zhang, J., Li, H.Y., Li, W.J., Li, M., Gu, R.R., Jiang, Y., Shan, Y., Gao, X.M., Liu, H.D., Guo, Z.X., Xue, L.K., Wang, W.X., 2020. Light absorption properties, absorption contributions, and the influencing factors of atmospheric brown carbon on Mount Tai. Geochimica 49, 262–272.
Epstein, S.A., Blair, S.L., Nizkorodov, S.A., 2014. Direct photolysis of alpha-pinene ozonolysis secondary organic aerosol: effect on particle mass and peroxide content. Environ. Sci. Technol. 48, 11251–11258. https://doi.org/10.1021/es502350u.
Farmer, D.K., Perring, A.E., Wooldridge, P.J., Blake, D.R., Baker, A., Meinardi, S., Huey, L.G., Tanner, D., Vargas, O., Cohen, R.C., 2011. Impact of organic nitrates on urban ozone production. Atmos. Chem. Phys. 11, 4085–4094. https://doi.org/10.5194/acp-11-4085-2011.
Fountoukis, C., Nenes, A., 2007. ISORROPIA II: a computationally efficient thermodynamic equilibrium model for K^+-Ca^{2+}-Mg^{2+}-NH_4^+-Na^+-SO_4^{2-}-NO_3^--Cl^--H_2O aerosols. Atmos. Chem. Phys. 7, 4639–4659. https://doi.org/10.5194/acp-7-4639-2007.
Fry, J.L., Brown, S.S., Middlebrook, A.M., Edwards, P.M., Campuzano-Jost, P., Day, D.A., Jimenez, J.L., Allen, H.M., Ryerson, T.B., Pollack, I., Graus, M., Warneke, C., de Gouw, J.A., Brock, C.A., Gilman, J., Lerner, B.M., Dube, W.P., Liao, J., Welti, A., 2018. Secondary organic aerosol (SOA) yields from NO_3 radical + isoprene based on nighttime aircraft power plant plume transects. Atmos. Chem. Phys. 18, 11663–11682. https://doi.org/10.5194/acp-18-11663-2018.
Fry, J.L., Draper, D.C., Zarzana, K.J., Campuzano-Jost, P., Day, D.A., Jimenez, J.L., Brown, S.S., Cohen, R.C., Kaser, L., Hansel, A., Cappellin, L., Karl, T., Roux, A.H., Turnipseed, A., Cantrell, C., Lefer, B.L., Grossberg, N., 2013. Observations of gas- and aerosol-phase organic nitrates at BEACHON-RoMBAS 2011. Atmos. Chem. Phys. 13, 8585–8605. https://doi.org/10.5194/acp-13-8585-2013.
Fry, J.L., Kiendler-Scharr, A., Rollins, A.W., Wooldridge, P.J., Brown, S.S., Fuchs, H., Dube, W., Mensah, A., dal Maso, M., Tillmann, R., Dorn, H.P., Brauers, T., Cohen, R. C., 2009. Organic nitrate and secondary organic aerosol yield from NO_3 oxidation of beta-pinene evaluated using a gas-phase kinetics/aerosol partitioning model. Atmos. Chem. Phys. 9, 1431–1449. https://doi.org/10.5194/acp-9-1431-2009.
Han, Y., Stroud, C.A., Liggio, J., Li, S.-M., 2016. The effect of particle acidity on secondary organic aerosol formation from α-pinene photooxidation under atmospherically relevant conditions. Atmos. Chem. Phys. 16, 13929–13944. https://doi.org/10.5194/acp-16-13929-2016.
Hewitt, C.N., 2001. The atmospheric chemistry of sulphur and nitrogen in power station plumes. Atmos. Environ. 35, 1155–1170. https://doi.org/10.1016/S1352-2310(00)00463-5.
Hlawiczka, S., Korszun, K., Fudala, J., 2016. Acidity of vapor plume from cooling tower mixed with flue gases emitted from coal-fired power plant. Sci. Total Environ. 554–555, 253–258. https://doi.org/10.1016/j.scitotenv.2016.02.172.
Hu, W.W., Hu, M., Hu, W., Jimenez, J.L., Yuan, B., Chen, W.T., Wang, M., Wu, Y.S., Chen, C., Wang, Z.B., Peng, J.F., Zeng, L.M., Shao, M., 2016. Chemical composition, sources, and aging process of submicron aerosols in Beijing: contrast between summer and winter. J. Geophys. Res. Atmos. 121, 1955–1977. https://doi.org/10.1002/2015jd024020.
Huang, H.L., Chao, W., Lin, J.J., 2015. Kinetics of a Criegee intermediate that would survive high humidity and may oxidize atmospheric SO_2. Proc. Natl. Acad. Sci. U.S. A. 112, 10857–10862. https://doi.org/10.1073/pnas.1513149112.
Huang, W., Yang, Y., Wang, Y., Gao, W., Li, H., Zhang, Y., Li, J., Zhao, S., Yan, Y., Ji, D., Tang, G., Liu, Z., Wang, L., Zhang, R., Wang, Y., 2021. Exploring the inorganic and organic nitrate aerosol formation regimes at a suburban site on the North China Plain. Sci. Total Environ. 768, 144538 https://doi.org/10.1016/j.scitotenv.2020.144538.
Jiang, L., Xu, Y.S., Ding, A.Z., 2010. Reaction of stabilized Criegee intermediates from ozonolysis of limonene with sulfur dioxide: ab initio and DFT study. J. Phys. Chem. 114, 12452–12461. https://doi.org/10.1021/jp107783z.
Jiang, Y., Xue, L.K., Gu, R.R., Jia, M.W., Zhang, Y.N., Wen, L., Zheng, P.G., Chen, T.S., Li, H.Y., Shan, Y., Zhao, Y., Guo, Z.X., Bi, Y.J., Liu, H.D., Ding, A.J., Zhang, Q.Z., Wang, W.X., 2020. Sources of nitrous acid (HONO) in the upper boundary layer and lower free troposphere of the North China Plain: insights from the Mount Tai Observatory. Atmos. Chem. Phys. 20, 12115–12131. https://doi.org/10.5194/acp-20-12115-2020.
Khan, M.A.H., Percival, C.J., Caravan, R.L., Taatjes, C.A., Shallcross, D.E., 2018. Criegee intermediates and their impacts on the troposphere. Environ. Sci.: Process. Impacts 20, 437–453. https://doi.org/10.1039/c7em00585g.
Kiendler-Scharr, A., Mensah, A.A., Friese, E., Topping, D., Nemitz, E., Prevot, A.S.H., Aijala, M., Allan, J., Canonaco, F., Canagaratna, M., Carbone, S., Crippa, M., Dall Osto, M., Day, D.A., De Carlo, P., Di Marco, C.F., Elbern, H., Eriksson, A., Freney, E., Hao, L., Herrmann, H., Hildebrandt, L., Hillamo, R., Jimenez, J.L., Laaksonen, A., McFiggans, G., Mohr, C., O'Dowd, C., Otjes, R., Ovadnevaite, J., Pandis, S.N., Poulain, L., Schlag, P., Sellegri, K., Swietlicki, E., Tiitta, P., Vermeulen, A., Wahner, A., Worsnop, D., Wu, H.C., 2016. Ubiquity of organic nitrates from nighttime chemistry in the European submicron aerosol. Geophys. Res. Lett. 43, 7735–7744. https://doi.org/10.1002/2016gl069239.
Kortelainen, A., Hao, L.Q., Tiitta, P., Jaatinen, A., Miettinen, P., Kulmala, M., Smith, J.N., Laaksonen, A., Worsnop, D.R., Virtanen, A., 2017. Sources of particulate organic nitrates in the boreal forest in Finland. Boreal Environ. Res. 22, 13–26.
Lee, A.K.Y., Adam, M.G., Liggio, J., Li, S.M., Li, K., Willis, M.D., Abbatt, J.P.D., Tokarek, T.W., Odame-Ankrah, C.A., Osthoff, H.D., Strawbridge, K., Brook, J.R., 2019. A large contribution of anthropogenic organo-nitrates to secondary organic aerosol in the Alberta oil sands. Atmos. Chem. Phys. 19, 12209–12219. https://doi.org/10.5194/acp-19-12209-2019.
Lee, B.H., Mohr, C., Lopez-Hilfiker, F.D., Lutz, A., Hallquist, M., Lee, L., Romer, P., Cohen, R.C., Iyer, S., Kurten, T., Hu, W., Day, D.A., Campuzano-Jost, P., Jimenez, J. L., Xu, L., Ng, N.L., Guo, H., Weber, R.J., Wild, R.J., Brown, S.S., Koss, A., de Gouw, J., Olson, K., Goldstein, A.H., Seco, R., Kim, S., McAvey, K., Shepson, P.B., Starn, T., Baumann, K., Edgerton, E.S., Liu, J., Shilling, J.E., Miller, D.O., Brune, W., Schobesberger, S., D'Ambro, E.L., Thornton, J.A., 2016. Highly functionalized organic nitrates in the southeast United States: contribution to secondary organic aerosol and reactive nitrogen budgets. Proc. Natl. Acad. Sci. U.S.A. 113, 1516–1521. https://doi.org/10.1073/pnas.1508108113.
Li, J.L., Li, H., Li, K., Chen, Y., Zhang, H., Zhang, X., Wu, Z.H., Liu, Y.C., Wang, X.Z., Wang, W.G., Ge, M.F., 2021a. Enhanced secondary organic aerosol formation from the photo-oxidation of mixed anthropogenic volatile organic compounds. Atmos. Chem. Phys. 21, 7773–7789. https://doi.org/10.5194/acp-21-7773-2021.
Li, R., Wang, X.F., Gu, R.R., Lu, C.Y., Zhu, F.P., Xue, L.K., Xie, H.J., Du, L., Chen, J.M., Wang, W.X., 2018. Identification and semi-quantification of biogenic organic nitrates in ambient particulate matters by UHPLC/ESI-MS. Atmos. Environ. 176, 140–147. https://doi.org/10.1016/j.atmosenv.2017.12.038.
Li, W., Huang, S., Yuan, B., Guo, S., Shao, M., 2021b. Mechanism,measurement techniques and their application for particulate organonitrates. China Environ. Sci. 41, 3017–3028.
Mahilang, M., Deb, M.K., Pervez, S., Tiwari, S., Jain, V.K., 2021. Biogenic secondary organic aerosol formation in an urban area of eastern central India: seasonal variation, size distribution and source characterization. Environ. Res. 195 https://doi.org/10.1016/j.envres.2021.110802.
Mao, J.Q., Paulot, F., Jacob, D.J., Cohen, R.C., Crounse, J.D., Wennberg, P.O., Keller, C. A., Hudman, R.C., Barkley, M.P., Horowitz, L.W., 2013. Ozone and organic nitrates over the eastern United States: sensitivity to isoprene chemistry. J. Geophys. Res. Atmos. 118, 11256–11268. https://doi.org/10.1002/jgrd.50817.
McGlynn, D.F., Barry, L.E.R., Lerdau, M.T., Pusede, S.E., Isaacman-VanWertz, G., 2021. Measurement report: variability in the composition of biogenic volatile organic compounds in a Southeastern US forest and their role in atmospheric reactivity. Atmos. Chem. Phys. 21, 15755–15770. https://doi.org/10.5194/acp-21-15755-2021.
Ng, N.L., Brown, S.S., Archibald, A.T., Atlas, E., Cohen, R.C., Crowley, J.N., Day, D.A., Donahue, N.M., Fry, J.L., Fuchs, H., Griffin, R.J., Guzman, M.I., Herrmann, H., Hodzic, A., Iinuma, Y., Jimenez, J.L., Kiendler-Scharr, A., Lee, B.H., Luecken, D.J., Mao, J., McLaren, R., Mutzel, A., Osthoff, H.D., Ouyang, B., Picquet-Varrault, B., Platt, U., Pye, H.O.T., Rudich, Y., Schwantes, R.H., Shiraiwa, M., Stutz, J., Thornton, J.A., Tilgner, A., Williams, B.J., Zaveri, R.A., 2017. Nitrate radicals and biogenic volatile organic compounds: oxidation, mechanisms, and organic aerosol. Atmos. Chem. Phys. 17, 2103–2162. https://doi.org/10.5194/acp-17-2103-2017.
Northcross, A.L., Jang, M., 2007. Heterogeneous SOA yield from ozonolysis of monoterpenes in the presence of inorganic acid. Atmos. Environ. 41, 1483–1493. https://doi.org/10.1016/j.atmosenv.2006.10.009.
Novelli, A., Hens, K., Ernest, C.T., Martinez, M., Nolscher, A.C., Sinha, V., Paasonen, P., Petaja, T., Sipila, M., Elste, T., Plass-Dulmer, C., Phillips, G.J., Kubistin, D., Williams, J., Vereecken, L., Lelieveld, J., Harder, H., 2017. Estimating the atmospheric concentration of Criegee intermediates and their possible interference in a FAGE-LIF instrument. Atmos. Chem. Phys. 17, 7807–7826. https://doi.org/10.5194/acp-17-7807-2017.
Perraud, V., Bruns, E.A., Ezell, M.J., Johnson, S.N., Greaves, J., Finlayson-Pitts, B.J., 2010. Identification of organic nitrates in the NO3 radical initiated oxidation of alpha-pinene by atmospheric pressure chemical ionization mass spectrometry. Environ. Sci. Technol. 44, 5887–5893. https://doi.org/10.1021/es1005658.
Perring, A.E., Pusede, S.E., Cohen, R.C., 2013. An observational perspective on the atmospheric impacts of alkyl and multifunctional nitrates on ozone and secondary organic aerosol. Chem. Rev. 113, 5848–5870. https://doi.org/10.1021/cr300520x.
Riedel, T.P., Lin, Y.H., Budisulistiorini, H., Gaston, C.J., Thornton, J.A., Zhang, Z.F., Vizuete, W., Gold, A., Surrattt, J.D., 2015. Heterogeneous reactions of isoprene-derived epoxides: reaction probabilities and molar secondary organic aerosol yield estimates. Environ. Sci. Technol. Lett. 2, 38–42. https://doi.org/10.1021/ez500406f.
Rindelaub, J.D., Borca, C.H., Hostetler, M.A., Slade, J.H., Lipton, M.A., Slipchenko, L.V., Shepson, P.B., 2016. The acid-catalyzed hydrolysis of an alpha-pinene-derived organic nitrate: kinetics, products, reaction mechanisms, and atmospheric impact.

Atmos. Chem. Phys. 16, 15425–15432. https://doi.org/10.5194/acp-16-15425-2016.

Rollins, A.W., Browne, E.C., Min, K.E., Pusede, S.E., Wooldridge, P.J., Gentner, D.R., Goldstein, A.H., Liu, S., Day, D.A., Russell, L.M., Cohen, R.C., 2012. Evidence for NO (x) control over nighttime SOA formation. Science 337, 1210–1212. https://doi.org/10.1126/science.1221520.

Rollins, A.W., Pusede, S., Wooldridge, P., Min, K.E., Gentner, D.R., Goldstein, A.H., Liu, S., Day, D.A., Russell, L.M., Rubitschun, C.L., Surratt, J.D., Cohen, R.C., 2013. Gas/particle partitioning of total alkyl nitrates observed with TD-LIF in Bakersfield. J. Geophys. Res. Atmos. 118, 6651–6662. https://doi.org/10.1002/jgrd.50522.

Sun, L., Xue, L.K., Wang, T., Gao, J., Ding, A.J., Cooper, O.R., Lin, M.Y., Xu, P.J., Wang, Z., Wang, X.F., Wen, L., Zhu, Y.H., Chen, T.S., Yang, L.X., Wang, Y., Chen, J. M., Wang, W.X., 2016. Significant increase of summertime ozone at mount Tai in central eastern China. Atmos. Chem. Phys. 16, 10637–10650. https://doi.org/10.5194/acp-16-10637-2016.

Takeuchi, M., Ng, N.L., 2019. Chemical composition and hydrolysis of organic nitrate aerosol formed from hydroxyl and nitrate radical oxidation of α-pinene and β-pinene. Atmos. Chem. Phys. 19, 12749–12766. https://doi.org/10.5194/acp-19-12749-2019.

Tegen, I., Schepanski, K., 2018. Climate feedback on aerosol emission and atmospheric concentrations. Curr. Clim. Change Rep. 4, 1–10. https://doi.org/10.1007/s40641-018-0086-1.

Turpin, B.J., Huntzicker, J.J., 1995. Identification of secondary organic aerosol episodes and quantitation of primary and secondary organic aerosol concentrations during Scaqs. Atmos. Environ. 29, 3527–3544. https://doi.org/10.1016/1352-2310(94)00276-Q.

Twomey, S.A., Piepgrass, M., Wolfe, T.L., 1984. An assessment of the impact of pollution on global cloud Albedo. Tellus Ser. B Chem. Phys. Meteorol. 36, 356–366. https://doi.org/10.1111/j.1600-0889.1984.tb00254.x.

Wang, Z., Wang, W.H., Tham, Y.J., Li, Q.Y., Wang, H., Wen, L., Wang, X.F., Wang, T., 2017. Fast heterogeneous N2O5 uptake and ClNO2 production in power plant and industrial plumes observed in the nocturnal residual layer over the North China Plain. Atmos. Chem. Phys. 17, 12361–12378. https://doi.org/10.5194/acp-17-12361-2017.

Welz, O., Savee, J.D., Osborn, D.L., Vasu, S.S., Percival, C.J., Shallcross, D.E., Taatjes, C. A., 2012. Direct kinetic measurements of Criegee intermediate (CH(2)OO) formed by reaction of CH(2)I with O(2). Science 335, 204–207. https://doi.org/10.1126/science.1213229.

Wen, L., Xue, L.K., Wang, X.F., Xu, C.H., Chen, T.S., Yang, L.X., Wang, T., Zhang, Q.Z., Wang, W.X., 2018. Summertime fine particulate nitrate pollution in the North China Plain: increasing trends, formation mechanisms and implications for control policy. Atmos. Chem. Phys. 18, 11261–11275. https://doi.org/10.5194/acp-18-11261-2018.

Xu, L., Suresh, S., Guo, H., Weber, R.J., Ng, N.L., 2015. Aerosol characterization over the southeastern United States using high-resolution aerosol mass spectrometry: spatial and seasonal variation of aerosol composition and sources with a focus on organic nitrates. Atmos. Chem. Phys. 15, 7307–7336. https://doi.org/10.5194/acp-15-7307-2015.

Xu, Y., Miyazaki, Y., Tachibana, E., Sato, K., Ramasamy, S., Mochizuki, T., Sadanaga, Y., Nakashima, Y., Sakamoto, Y., Matsuda, K., Kajii, Y., 2020. Aerosol liquid water promotes the formation of water-soluble organic nitrogen in submicrometer aerosols in a suburban forest. Environ. Sci. Technol. 54, 1406–1414. https://doi.org/10.1021/acs.est.9b05849.

Yao, L., Yang, L., Chen, J., Wang, X., Xue, L., Li, W., Sui, X., Wen, L., Chi, J., Zhu, Y., Zhang, J., Xu, C., Zhu, T., Wang, W., 2016. Characteristics of carbonaceous aerosols: impact of biomass burning and secondary formation in summertime in a rural area of the North China Plain. Sci. Total Environ. 557–558, 520–530. https://doi.org/10.1016/j.scitotenv.2016.03.111.

Ye, J.H., Abbatt, J.P.D., Chan, A.W.H., 2018. Novel pathway of SO_2 oxidation in the atmosphere: reactions with monoterpene ozonolysis intermediates and secondary organic aerosol. Atmos. Chem. Phys. 18, 5549–5565. https://doi.org/10.5194/acp-18-5549-2018.

Yu, K.Y., Zhu, Q., Du, K., Huang, X.F., 2019. Characterization of nighttime formation of particulate organic nitrates based on high-resolution aerosol mass spectrometry in an urban atmosphere in China. Atmos. Chem. Phys. 19, 5235–5249. https://doi.org/10.5194/acp-19-5235-2019.

Zare, A., Romer, P.S., Nguyen, T., Keutsch, F.N., Skog, K., Cohen, R.C., 2018. A comprehensive organic nitrate chemistry: insights into the lifetime of atmospheric organic nitrates. Atmos. Chem. Phys. 18, 15419–15436. https://doi.org/10.5194/acp-18-15419-2018.

Zhang, J., Wang, X.F., Li, R., Dong, S.W., Chen, J., Zhang, Y.N., Zheng, P.G., Li, M., Chen, T.S., Liu, Y.H., Xue, L.K., Zhou, X.H., Du, L., Zhang, Q.Z., Wang, W.X., 2021. Significant impacts of anthropogenic activities on monoterpene and oleic acid-derived particulate organic nitrates in the North China Plain. Atmos. Res. 256 https://doi.org/10.1016/j.atmosres.2021.105585.

Zhang, J., Wang, X.F., Zhang, Y.N., Gu, R.R., Xia, M., Li, H., Dong, S.W., Xue, L.K., Wu, Z. H., Zhang, Y.J., Gao, J., Wang, T., Wang, W.X., 2020. Pollution characteristics and formation of particulate organic nitrates in winter in Beijing City. Geochimica 49, 252–261.

Zhang, J.K., Cheng, M.T., Ji, D.S., Liu, Z.R., Hu, B., Sun, Y., Wang, Y.S., 2016. Characterization of submicron particles during biomass burning and coal combustion periods in Beijing, China. Sci. Total Environ. 562, 812–821. https://doi.org/10.1016/j.scitotenv.2016.04.015.